



Absorption-edge anisotropy of $\text{Cu}_2\text{ZnSiQ}_4$ ($Q = \text{S}, \text{Se}$) quaternary compound semiconductors

S. Levenco^{a,1}, D. Dumcenco^{a,1}, Y.S. Huang^{a,*}, E. Arushanov^b, V. Tezlevan^b, K.K. Tiong^c, C.H. Du^d

^a Department of Electronic Engineering, National Taiwan University of Science and Technology, Taipei 106, Taiwan

^b Institute of Applied Physics, Academy of Sciences of Moldova, Chisinau MD 2028, Republic of Moldova

^c Department of Electrical Engineering, National Taiwan Ocean University, Keelung 202, Taiwan

^d Department of Physics, Tamkang University, Tamsui 251, Taiwan

ARTICLE INFO

Article history:

Received 20 August 2010

Accepted 30 January 2011

Available online 24 February 2011

PACS:

78.20.ci

78.40.-q

78.40.Fy

Keywords:

Semiconductors

Optical properties

Optical spectroscopy

ABSTRACT

Polarization-dependent absorption characterization of $\text{Cu}_2\text{ZnSiQ}_4$ ($Q = \text{S}, \text{Se}$) quaternary single crystal compound semiconductors were carried out in the temperature range of 10–300 K. The absorption measurements were performed on the as grown basal plane with the normal along $[2\ 1\ 0]$ and the axis c parallel to the long edge of the crystal platelet. A significant shift towards lower energy was observed in the absorption spectra of $E \perp c$ polarization with respect to those corresponding to $E \parallel c$ polarization. A comprehensive analysis of the absorption spectra revealed that the absorption edges of the studied crystals are indirect allowed transitions. A schematic representation of the plausible assignments for the observed near band edge optical transitions for $\text{Cu}_2\text{ZnSiQ}_4$ was proposed. The variation of the indirect transition energies with temperature were analyzed by Varshni and Bose–Einstein expressions. The parameters that describe the temperature dependence of the indirect transition energies with different polarizations were evaluated and discussed.

© 2011 Elsevier B.V. All rights reserved.

1. Introduction

$\text{Cu}_2\text{ZnSiQ}_4$ ($Q = \text{S}, \text{Se}$) belong to the family of Cu-based quaternary chalcogenide compounds, $\text{Cu}_2\text{-II-IV-VI}_4$, crystallizing in the wurtz-stannite structure with space group $Pmn2_1$ [1–3]. The structure of $\text{Cu}_2\text{ZnSiQ}_4$ consists of alternating cation layers of mixed Zn and Si atoms separated by layers of Cu atoms. It is therefore derived from an ordering of the cations of the wurtzite cell. In these compounds each sulfur/selenium atom has four nearest neighbor cation atoms (two copper atoms, one zinc atom, and a silicon atom) at the corners of the surrounding tetrahedron [1–3]. These materials are of interest for its nonlinear optical properties [4,5] and potential for high-temperature thermoelectric [6] and optoelectronics [7] applications. Despite their interesting optical and thermoelectric properties, and possible applications, up-to-date, only a few studies have been reported concerning the basic properties of $\text{Cu}_2\text{ZnSiQ}_4$, due to the difficulty of preparing suitable size, compositionally homogeneous and high purity single crystals. Among those studies, some discrepancies have been reported [8,9].

In this paper, we report on a detailed polarization-dependent optical-absorption study of $\text{Cu}_2\text{ZnSiS}_4$ and $\text{Cu}_2\text{ZnSiSe}_4$ single crystals over the temperature range from 10 to 300 K. High quality single crystals of $\text{Cu}_2\text{ZnSiS}_4$ and $\text{Cu}_2\text{ZnSiSe}_4$ were grown by chemical vapor transport using iodine as the transport agent. The absorption measurements were carried out on the as grown basal plane with the normal along $[2\ 1\ 0]$ and the axis c parallel to the long edge of the crystal platelet. Analysis of the absorption curves revealed that the interband transitions in $\text{Cu}_2\text{ZnSiS}_4$ and $\text{Cu}_2\text{ZnSiSe}_4$ are indirect and their band gaps are polarization dependent. The polarization-dependent energy gaps of these materials at various temperatures were determined and their temperature dependences were analyzed by the Varshni equation [10] and an expression containing the Bose–Einstein occupation factor for phonons [11]. The parameters that describe the temperature dependence of band gaps were evaluated and discussed.

2. Experimental

Single crystals of $\text{Cu}_2\text{ZnSiS}_4$ and $\text{Cu}_2\text{ZnSiSe}_4$ were grown by vapor transport of stoichiometric amounts of the elements with 5 mg iodine/cm³ as the transport agent. Optimum crystal growth was achieved with the charge zone maintained at 850 °C and the growth zone at 800 °C. The transport process was carried out for a period of 14 days. Single crystals $\text{Cu}_2\text{ZnSiS}_4$ ($\text{Cu}_2\text{ZnSiSe}_4$) formed thin, greenish (orange), blade shape up to 10 mm × 1.5 mm (20 mm × 1.0 mm) in area and 300 (100) μm in thickness. The orientation of the basal plane was determined by comparing back-reflection Laue pattern with computer generated Laue plots. With the

* Corresponding author. Tel.: +886 2 27376385; fax: +886 2 27376424.

E-mail address: ysh@mail.ntust.edu.tw (Y.S. Huang).

¹ Present address: Institute of Applied Physics, Academy of Sciences of Moldova, Chisinau MD 2028, Republic of Moldova.

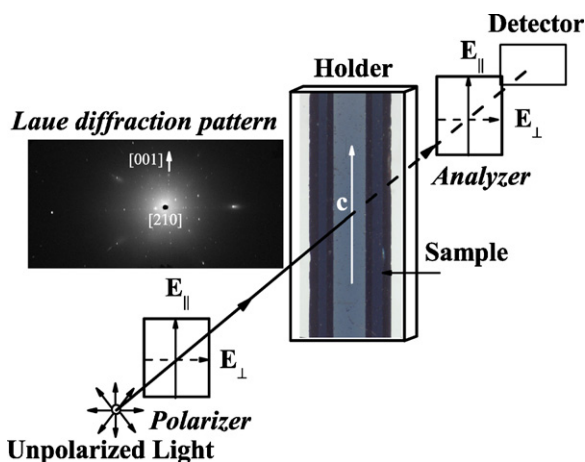


Fig. 1. A schematic arrangement of the polarization-dependent absorption measurements on $\text{Cu}_2\text{ZnSiQ}_4$ compound semiconductors.

X-ray beam normal to the basal plane, the Laue pattern displayed a twofold asymmetry pattern (see Fig. 1). Analyzing the symmetry of Laue pattern confirms the formation of orthorhombic structure and reveal that the normal of the basal plane is $[2\ 1\ 0]$ and the long-edge of the crystal platelet is parallel to c -axis.

For the transmittance measurements, single crystals with a thickness of about $100\ \mu\text{m}$ were used. Plate-shaped crystals were selected and mounted on a copper sample holder. Fig. 1 depicts the schematic arrangement of the polarization-dependent transmittance measurements with polarization configurations of $E_{\perp c}$ and $E_{\parallel c}$ performed on the as grown basal plane with the normal along $[2\ 1\ 0]$ and c parallel to the long edge of the crystal platelet. A 150W xenon arc lamp filtered by a 0.25m grating monochromator provided the source for optical measurements. Model PRH 8020 CASIX Rochon prisms were employed for polarization dependent measurements. An UV enhanced Si detector was used to detect the transmitted or reflected signals. Measurements of the reflectivity and transmission at near-normal incidence configuration with chopped light were carried out. For temperature dependent measurements, a closed-cycle cryogenic refrigerator equipped with a digital thermometer controller was used for the low temperature measurements with a temperature stability of 0.5K or better.

3. Results and discussion

The transmittance of $\text{Cu}_2\text{ZnSiS}_4$ and $\text{Cu}_2\text{ZnSiSe}_4$ were measured at near-normal incidence. The absorption coefficient α was determined from the transmittance T_r by taking into account the spectral dependence of the reflectance R using the relation [12]:

$$T_r = \frac{(1 - R)^2 e^{-\alpha d}}{1 - R^2 e^{-2\alpha d}} \quad (1)$$

Eq. (1) assumes multiple reflections within the sample, but that they add incoherently due to sample inhomogeneity or a sufficiently large spread of the incident angles. Since αd is large for the sample crystals, the second term in the denominator of Eq. (1) can be neglected.

Fig. 2 displays the absorption coefficient α as a function of photon energy, as determined $\text{Cu}_2\text{ZnSiS}_4$ and $\text{Cu}_2\text{ZnSiSe}_4$, at (a) 10 and (b) 300 K. The dash-dotted curves in Fig. 2 correspond to the $E_{\parallel c}$ polarization, while the solid curves represent $E_{\perp c}$ polarization. It is noted that a significant shift towards lower energy for the $E_{\perp c}$ polarization is observed as compared to the $E_{\parallel c}$ polarization. The polarization dependence of the transmittance curves provides conclusive evidence that both optical absorption edges are associated with the interband transitions from different origins. Detailed theoretical study of the anisotropic optical properties in the basal plane with the normal along $[2\ 1\ 0]$ of $\text{Cu}_2\text{ZnSiS}_4$ and $\text{Cu}_2\text{ZnSiSe}_4$ is needed and is at present beyond the scope of this work. As is generally expected, the absorption edge shifted towards higher energies as the temperature of the sample is lowered from 300 to 10 K. Analysis of the experimental data showed that the absorp-

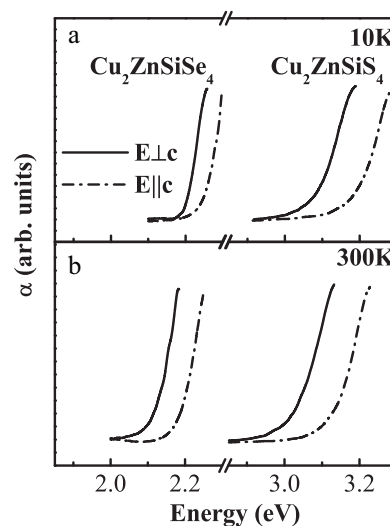


Fig. 2. The $E_{\perp c}$ polarization and $E_{\parallel c}$ polarization absorption spectra of $\text{Cu}_2\text{ZnSiS}_4$ and $\text{Cu}_2\text{ZnSiSe}_4$ at (a) 10 and (b) 300 K. The dash-dotted curves in correspond to the $E_{\parallel c}$ polarization, while the solid curves represent $E_{\perp c}$ polarization.

tion coefficient α to be proportional to $(h\nu - E_g)^n$ with $n \approx 2$. This suggests an indirect allowed transition for these materials.

A more complete analysis, taking into accounts both the absorption and emission phonons, is given as follows. For an indirect allowed transition, the absorption coefficient α for a single-phonon process can be expressed as [13]:

$$\alpha h\nu = \frac{A(h\nu - E_g + E_p)^2}{\exp(E_p/kT) - 1} + \frac{B(h\nu - E_g - E_p)^2}{1 - \exp(-E_p/kT)} \quad (2)$$

where $h\nu$ is the energy of the incident photon, E_g is the band gap, E_p is the energy of the phonon assisting the transition, and A and B are constants. The first term on the right-hand side of Eq. (2) corresponds to an absorption of a photon and a phonon, whereas the second term corresponds to an absorption of a photon and emission of a phonon which contributes only when $h\nu \geq E_g + E_p$. There is a large residual absorption at photon energies below the absorption edge. The large values of the absorption coefficient α below the absorption edge of $\text{Cu}_2\text{ZnSiS}_4$ and $\text{Cu}_2\text{ZnSiSe}_4$ most probably indicate the existence of impurities or defects in the materials. At this point, we have not considered in detail the effect of these impurity or defect states. For simplicity, in our present study, the residual absorption is assumed to be a constant and subtracted out for the evaluation of the band gap E_g and phonon energy E_p . The data of $\text{Cu}_2\text{ZnSiS}_4$ and $\text{Cu}_2\text{ZnSiSe}_4$ at different temperatures were then fitted to Eq. (2). Representative results are shown in Figs. 3 and 4 for $\text{Cu}_2\text{ZnSiS}_4$ and $\text{Cu}_2\text{ZnSiSe}_4$, respectively, where the open-circles and triangles are representative experimental points deduced from $E_{\perp c}$ and $E_{\parallel c}$ polarizations absorption spectra and the solid lines are fitted to Eq. (2). The obtained values of the indirect band gaps and phonon energies at 10 and 300 K are listed in Table 1. The results strongly indicate that $\text{Cu}_2\text{ZnSiS}_4$ and $\text{Cu}_2\text{ZnSiSe}_4$ are indirect transition semiconductors, in which $E_{\perp c}$ polarization exhibits a smaller band gap and a single phonon makes important contributions in assisting the indirect transitions. The nonuniform thicknesses and unsmooth sample surfaces will cause some deviations of the incident angles from the normal direction, resulting in some variations in the absorption spectra. Differing values of E_g and E_p could be obtained by fitting a different energy range, i.e. by inclusion or exclusion of some points at lower or higher photon energies. From this selective omission of data, an error of the order $\pm 0.01\ \text{eV}$ ($\pm 0.02\ \text{eV}$) and ± 5 (± 5) meV can be deduced for the determination of E_g and E_p , respectively, at 10 (300) K. Fitting data on different

Table 1
Values of the indirect transition energies $E_{g\perp}^{ind}$ and $E_{g\parallel}^{ind}$ and phonon energy E_p of $\text{Cu}_2\text{ZnSiS}_4$ and $\text{Cu}_2\text{ZnSiSe}_4$ obtained by fitting absorption data to Eq. (2) at 10 and 300 K.

Materials	Temperature (K)	$E_{g\perp}^{ind}$ (eV)	E_p (meV)	$E_{g\parallel}^{ind}$ (eV)	E_p (meV)
$\text{Cu}_2\text{ZnSiS}_4$	10	3.00 ± 0.01	30 ± 5	3.10 ± 0.01	30 ± 5
	300	2.94 ± 0.02	30 ± 5	3.04 ± 0.02	30 ± 5
$\text{Cu}_2\text{ZnSiSe}_4$	10	2.15 ± 0.01	20 ± 5	2.20 ± 0.01	20 ± 5
	300	2.08 ± 0.02	20 ± 5	2.14 ± 0.02	20 ± 5

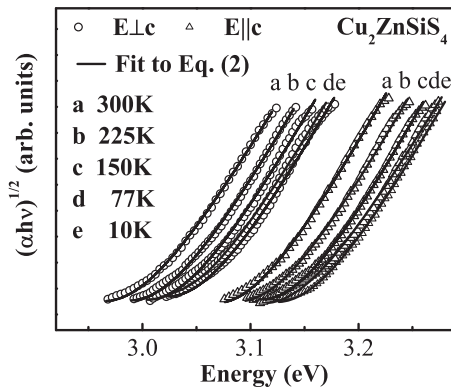


Fig. 3. Plots $(\alpha h\nu)^{1/2}$ as a function of the photon energy at different temperatures ranging from 10 to 300 K for $E_{\perp c}$ polarization (open circles) and $E_{\parallel c}$ polarization (open triangles) for $\text{Cu}_2\text{ZnSiS}_4$.

samples give similar parameters, even though there are differences in the absorption spectra due to differences in sample thicknesses.

As listed in Table 1, the indirect gaps for $E_{\perp c}$ ($E_{\parallel c}$) polarization denoted as $E_{g\perp}^{ind}$ ($E_{g\parallel}^{ind}$) and phonon energy E_p at room temperature, are, respectively, determined to be 2.94 ± 0.02 (3.04 ± 0.02) eV and 30 ± 5 meV for $\text{Cu}_2\text{ZnSiS}_4$ and 2.08 ± 0.02 (2.14 ± 0.02) eV and 20 ± 5 meV for $\text{Cu}_2\text{ZnSiSe}_4$. It is noticed that the values for $E_{g\parallel}^{ind}$ are larger than those of $E_{g\perp}^{ind}$, and are similar to E_g^{ind} determined from the absorption data of the unpolarized incident light. It is also noted that the difference between $E_{g\parallel}^{ind}$ and $E_{g\perp}^{ind}$ for $\text{Cu}_2\text{ZnSiS}_4$ (100 meV) is much larger than that of $\text{Cu}_2\text{ZnSiSe}_4$ (60 meV). Our values differ slightly from previous published works [8,9]. The first available data, 3.25 eV for $\text{Cu}_2\text{ZnSiS}_4$ and 2.33 eV for $\text{Cu}_2\text{ZnSiSe}_4$ were obtained by Schleich and Wold [8] from transmittance measurements. From optical-absorption measurements, Yao et al.

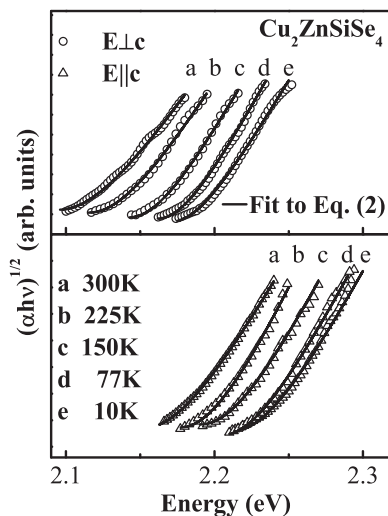


Fig. 4. Plots $(\alpha h\nu)^{1/2}$ as a function of the photon energy at different temperatures ranging from 10 to 300 K for $E_{\perp c}$ polarization (open-circles) and $E_{\parallel c}$ polarization (open-triangles) for $\text{Cu}_2\text{ZnSiSe}_4$.

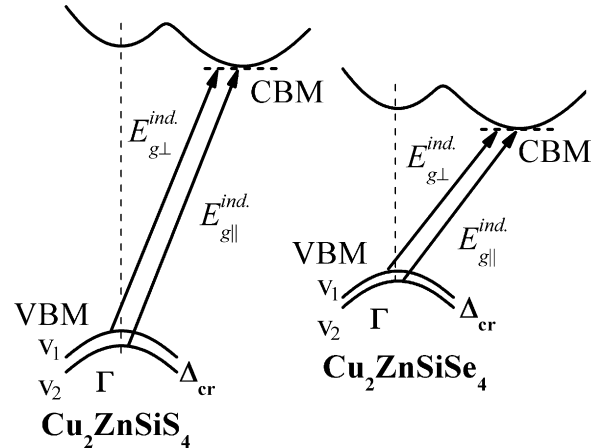


Fig. 5. A schematic representation of the plausible assignments for the observed optical transitions near indirect band edge for $\text{Cu}_2\text{ZnSiQ}_4$ compound semiconductors.

[9] determined the indirect optical band gaps of $\text{Cu}_2\text{ZnSiS}_4$ and $\text{Cu}_2\text{ZnSiSe}_4$ to be 3.04(2) eV and 2.20(2) eV, respectively.

In order to understand the obtained experimental results, a band diagram near the band edge is needed. Recently Chen et al reported a band-structure calculation on a family of wurtzite-derived polytypes of kesterite and stannite $\text{I}_2\text{-II-IV-VI}_4$ quaternary chalcogenide semiconductors [14]. From their calculation, the following results were shown: (i) $\text{I}_2\text{-II-IV-VI}_4$ semiconductors have usually direct band gaps at the Γ point, (ii) the top of the valence band is mainly the antibonding component of the p - d hybridization between the group-VI anion and group-I cation, (iii) the bottom of the conduction band is mainly the antibonding component of the s - s and s - p hybridization [15], except for those containing Si, the group-I and -II cations also have significant contribution to the bottom of the conduction band as well as Si and group-VI anion.

Adopting the band-structure calculation by Chen et al. [14] and our previous reported piezoreflectance spectra of $\text{Cu}_2\text{ZnSiS}_4$ [16,17] which exhibit a lower transition feature for $E_{\perp c}$ polarization and a distinctly higher transition for $E_{\parallel c}$ polarization, a schematic representation of the plausible assignments for the observed near band edge optical transitions for $\text{Cu}_2\text{ZnSiQ}_4$ is presented in Fig. 5. The energy of the transition depends strongly on the orientation of the polarization with respect to the crystallographic directions. Thus the difference between the $E_{\perp c}$ and $E_{\parallel c}$ levels of the valence band shown in Fig. 5 is attributed solely to the crystal field splitting for orthorhombic crystalline symmetry of $\text{Cu}_2\text{ZnSiQ}_4$ which is described by the space group $Pmn2_1$.

Plotted in Fig. 6 are the temperature variations of the polarization-dependent indirect energy gaps of $\text{Cu}_2\text{ZnSiS}_4$ and $\text{Cu}_2\text{ZnSiSe}_4$ with representative error bars. A least-squares fit (the solid line) to the Varshni semiempirical relationship [10]:

$$E_{g_i}^{ind}(T) = E_{g_i}^{ind}(0) - \frac{a_i T^2}{T + b_i} \quad (3)$$

yields parameters as given in Table 2. Here $i = \perp, \parallel$; $E_{g_i}^{ind}(0)$ is the indirect band gap at 0 K; a_i and b_i are constants referred to as Varshni

Table 2

Values of the Varshni and Bose–Einstein parameters of $\text{Cu}_2\text{ZnSiS}_4$ and $\text{Cu}_2\text{ZnSiSe}_4$ obtained by fitting the temperature-dependent data of indirect transition energies $E_{g,\perp}^{\text{ind}}$ and $E_{g,\parallel}^{\text{ind}}$ to Eqs. (3) and (4), respectively. The corresponding values for the direct excitonic transition energies of $\text{Cu}_2\text{ZnSiS}_4$ as well as indirect band gaps of Si, GaP, 4H-SiC are also listed for comparison.

Materials	Feature	$E(0)$ (eV)	a (10^{-4} eV/K)	b (K)	a_B (meV)	Θ_B (K)
$\text{Cu}_2\text{ZnSiS}_4$	$E_{g,\perp}^{\text{ind}}$ ^a	2.99 ± 0.01	4 ± 1	350 ± 150	60 ± 10	350 ± 40
	$E_{g,\parallel}^{\text{ind}}$ ^a	3.10 ± 0.01	4 ± 1	290 ± 140	60 ± 10	330 ± 50
$\text{Cu}_2\text{ZnSiSe}_4$	$E_{g,\perp}^{\text{ind}}$ ^a	2.15 ± 0.01	5 ± 1	270 ± 100	50 ± 10	250 ± 50
	$E_{g,\parallel}^{\text{ind}}$ ^a	2.20 ± 0.01	4 ± 1	260 ± 120	45 ± 10	300 ± 50
$\text{Cu}_2\text{ZnSiS}_4$	$E_{g,\perp}^{\text{exc}}$ ^b	3.390 ± 0.003	5 ± 1	380 ± 90	80 ± 10	370 ± 50
	$E_{g,\parallel}^{\text{exc}}$ ^b	3.481 ± 0.003	5 ± 1	350 ± 100	70 ± 10	340 ± 50
Si	E_g^{ind} ^c	1.17 ^c	4.7 ^c	636 ^c	19 ^d	296 ^d
GaP	E_g^{ind} ^e	2.338 ^e	6.2 ^e	460 ^e	73 ^d	506 ^d
4H-SiC	E_g^{ind} ^f	3.267 ^f	3.2 ^f	565 ^f		

^a Present work.

^b Ref. [17].

^c Ref. [18].

^d Ref. [21].

^e Ref. [19].

^f Ref. [20].

coefficients. The constant a_i is related to the electron–phonon interaction and b_i is closely related to the Debye temperature. The obtained values of b_i for $\text{Cu}_2\text{ZnSiSe}_4$ are found to be smaller than that of $\text{Cu}_2\text{ZnSiS}_4$ may indicate that the Debye temperature for selenium contented compound is lower than that of sulfur one. For comparison purposes, we have also listed numbers for the polarization-dependent direct band edge excitonic-transition energies of $\text{Cu}_2\text{ZnSiS}_4$ [17] and the indirect band edge of Si [18], GaP [19] and 4HSiC [20] in Table 2.

The temperature dependence of the indirect band edge transition energies $E_{g,\perp}^{\text{ind}}$ and $E_{g,\parallel}^{\text{ind}}$ can also be fitted (dash-dotted curve) by an expression containing the Bose–Einstein occupation factor for phonon [11]:

$$E_{gi}^{\text{ind}}(T) = E_{gi}^{\text{ind}}(0) - \frac{2a_{Bi}}{[\exp(\Theta_{Bi}/T) - 1]} \quad (4)$$

where $i = \perp$ or \parallel , $E_{gi}^{\text{ind}}(0)$ is the indirect band gap at 0 K, a_{Bi} represents the strength of the electron–phonon interaction, and Θ_{Bi} corresponds to the average phonon temperature. The fitted values for $E_{gi}^{\text{ind}}(0)$, a_{Bi} , and Θ_{Bi} are given in Table 2, and the corresponding

values for the polarization-dependent direct band edge excitonic-transition energies of $\text{Cu}_2\text{ZnSiS}_4$ [17], and the numbers deduced from the expression proposed by O'Donnel and Chen [21] for indirect band edge of Si and GaP are also listed in Table 2 for comparison. The fitted values of average phonon temperature of Θ_{Bi} for $\text{Cu}_2\text{ZnSiS}_4$ are found to be larger than that of $\text{Cu}_2\text{ZnSiSe}_4$. If we assume the force constants of S and Se contented compounds are similar, the difference of Θ_{Bi} may be attributed mainly to the mass difference between S and Se, where the heavier element, i.e. Se, yields a lower phonon temperature.

The parameter a_i in Eq. (3) can be related to a_{Bi} and Θ_{Bi} in Eq. (4) by taking the high-temperature limit of both expressions, which yields to $a_i \approx 2a_{Bi}/\Theta_{Bi}$. Comparison of the values presented in Table 2 shows that this relation is indeed satisfied. From Eq. (4) it is straightforward to show that the high temperature limit of the slope of $E_{gi}^{\text{ind}}(T)$ versus T curve approaches the value of $-2a_{Bi}/\Theta_{Bi}$. The calculated values of $-2a_{Bi}/\Theta_{Bi}$ for $E_{g,\perp}^{\text{ind}}$ and $E_{g,\parallel}^{\text{ind}}$ equal to -0.34 (0.40) and -0.36 (0.30) meV/K for $E_{\perp c}$ and $E_{\parallel c}$, respectively, which agree reasonably with the values of $dE_{g,\perp}^{\text{ind}}/dT = -0.32$ (0.35) meV/K and $dE_{g,\parallel}^{\text{ind}}/dT = -0.31$ (0.27) meV/K obtained from linear extrapolation in the higher temperature (200–300 K) absorption experimental data for $\text{Cu}_2\text{ZnSiS}_4$ ($\text{Cu}_2\text{ZnSiSe}_4$).

4. Summary

The temperature dependence of the indirect band-edge transitions of single crystals $\text{Cu}_2\text{ZnSiS}_4$ and $\text{Cu}_2\text{ZnSiSe}_4$ were characterized by using polarization-dependent absorption measurements in the temperature range between 10 and 300 K. The single crystals of $\text{Cu}_2\text{ZnSiS}_4$ and $\text{Cu}_2\text{ZnSiSe}_4$ were grown by chemical vapor transport technique using iodine as transport agent. The absorption measurements were carried out on the as-grown basal plane with the normal along $[2\ 1\ 0]$ and the c axis parallel to the long edge of the crystal platelet. A comprehensive analysis of the absorption spectra revealed polarization-dependent anisotropic indirect band gaps of $E_{g,\perp}^{\text{ind}}$ and $E_{g,\parallel}^{\text{ind}}$ for $E_{\perp c}$ and $E_{\parallel c}$ polarization, respectively. A schematic representation of the plausible assignments for the observed near band edge optical transitions for $\text{Cu}_2\text{ZnSiS}_4$ was presented. The differences of the indirect band gaps $E_{g,\perp}^{\text{ind}}$ and $E_{g,\parallel}^{\text{ind}}$ are attributed mainly due to the crystal field splitting at the Γ point of the valence band. The splitting for $\text{Cu}_2\text{ZnSiS}_4$ is found to be larger than that of $\text{Cu}_2\text{ZnSiSe}_4$. In addition, the temperature dependence of the indirect band gaps has been analyzed by both Varshni- and Bose–Einstein-type expressions. The parameters extracted from

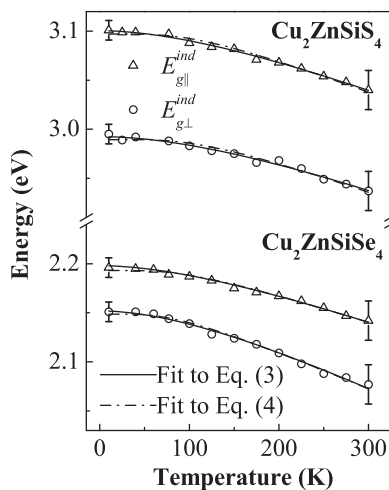


Fig. 6. Temperature dependence of the indirect gaps of $\text{Cu}_2\text{ZnSiS}_4$ and $\text{Cu}_2\text{ZnSiSe}_4$. The experimental results have been determined by fit of the absorption data to Eq. (2). The open-circles and triangles are energies of $E_{g,\perp}^{\text{ind}}$ and $E_{g,\parallel}^{\text{ind}}$ indirect transitions, respectively, with representative error bars. The solid and dash-dotted curves represent the calculated dependency according to the Varshni (Eq. (3)) and Bose–Einstein (Eq. (4)) expressions, respectively.

both expressions by extending into the high-temperature regime are found to agree reasonable well. Both the Debye temperature related parameters b_i and average phonon temperatures Θ_{Bi} for $\text{Cu}_2\text{ZnSiSe}_4$ are smaller than those of $\text{Cu}_2\text{ZnSiS}_4$.

Acknowledgments

The authors acknowledge the support of National Science Council of Taiwan under Project Nos. NSC 098-2811-E-011-019, NSC 97-2112-M-011-001-MY3 and 98-2221-E-011-015-MY2.

References

- [1] R. Nitsche, D.F. Sargent, P. Wild, J. Cryst. Growth 1 (1967) 52–53.
- [2] W. Schafer, R. Nitsche, Mater. Res. Bull. 9 (1974) 645–654.
- [3] H. Matsushita, T. Ichikawa, A. Katsui, J. Mater. Sci. 40 (2005) 2003–2005.
- [4] J.W. Lekse, M.A. Moreau, K.L. McNerny, J. Yeon, P.S. Halasyamani, J.A. Aitken, Inorg. Chem. 48 (2009) 7516–7518.
- [5] J.W. Lekse, B.M. Leverett, C.H. Lake, J.A. Aitken, J. Solid State Chem. 181 (2008) 3217–3222.
- [6] M.L. Liu, F.Q. Huang, L.D. Chen, I.W. Chen, Appl. Phys. Lett. 94 (2009) 202103 (3 pp.).
- [7] T. Oike, T. Iwasaki, AH01L2915FI, <http://www.faqs.org/patents/app/20080303035#ixzz0iW8PX6KV>.
- [8] D.M. Schleich, A. Wold, Mater. Res. Bull. 12 (1977) 111–114.
- [9] G.Q. Yao, H.S. Shen, E.D. Honig, R. Kershaw, K. Dwight, A. Wold, Solid State Ionics 24 (1987) 249–252.
- [10] Y.P. Varshni, Physica (Utrecht) 34 (1967) 149–154.
- [11] P. Lautenschlager, M. Garriga, S. Logothetidis, M. Cardona, Phys. Rev. B 35 (1987) 9174–9189.
- [12] J.S. Blakemore, K.C. Nomura, Phys. Rev. 127 (1962) 1024–1029.
- [13] J.I. Pankove, Optical Processes in Semiconductors, Dover, New York, 1975.
- [14] S. Chen, A. Walsh, Y. Luo, J.H. Yang, X.G. Gong, S.H. Wei, Phys. Rev. B 82 (2010) 195203 (8pp.).
- [15] S. Chen, X.G. Gong, A. Walsh, S.H. Wei, Phys. Rev. B 79 (2009) 165211 (10pp.).
- [16] S. Levenco, D. Dumcenco, Y.S. Huang, E. Arushanov, V. Tezlevan, K.K. Tiong, C.H. Du, J. Appl. Phys. 108 (2010) 073508 (5pp.).
- [17] S. Levenco, D. Dumcenco, Y.S. Huang, E. Arushanov, V. Tezlevan, K.K. Tiong, C.H. Du, J. Alloys Compd. 506 (2010) 46–50.
- [18] www.ioffe.rssi.ru/SVA/NSM/Semicond/Si/index.html.
- [19] M.B. Panish, H.C. Casey, J. Appl. Phys. 40 (1969) 163–167.
- [20] P. Grivickas, V. Grivickas, J. Linnros, A. Galeckas, J. Appl. Phys. 101 (2007) 123521 (10 pp.).
- [21] K.P. O'Donnel, X. Chen, Appl. Phys. Lett. 58 (1991) 2924–2926.